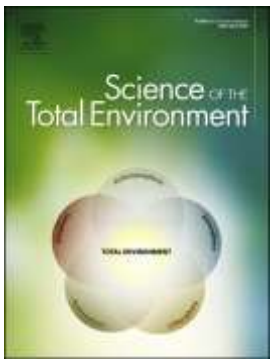

In vitro lung toxicity of indoor PM10 from a stove fueled with different biomasses

Sara Marchetti, Eleonora Longhin, Rossella Bengalli, Pasquale Avino, Luca Stabile, Giorgio Buonanno, Anita Colombo, Marina Camatini, Paride Mantecca

PII:	S0048-9697(18)33213-3
DOI:	doi:10.1016/j.scitotenv.2018.08.249
Reference:	STOTEN 28311
To appear in:	*Science of the Total Environment*
Received date:	11 June 2018
Revised date:	3 August 2018
Accepted date:	19 August 2018

Please cite this article as: Sara Marchetti, Eleonora Longhin, Rossella Bengalli, Pasquale Avino, Luca Stabile, Giorgio Buonanno, Anita Colombo, Marina Camatini, Paride Mantecca , In vitro lung toxicity of indoor PM10 from a stove fueled with different biomasses. Stoten (2018), doi:10.1016/j.scitotenv.2018.08.249

In vitro lung toxicity of indoor PM10 from a stove fueled with different biomasses

Sara Marchetti[a] *, Eleonora Longhin[a], Rossella Bengalli[a], Pasquale Avino[b], Luca Stabile[c], Giorgio Buonanno[c,d,e], Anita Colombo[a], Marina Camatini[a], Paride Mantecca[a].

[a]POLARIS Research Centre, Department of Earth and Environmental Sciences, University of Milano-Bicocca, Piazza della Scienza 1, 20126 Milano, Italy

[b]DiAAA, University of Molise, via De Sanctis, 86100 Campobasso, Italy

[c]Department of Civil and Mechanical Engineering, University of Cassino and Southern Lazio, Via Di Biasio 43, 03043 Cassino (FR) Italy

[d]University of Naples "Parthenope", Via Ammiraglio Ferdinando Acton, 38, 80133 Napoli, Italy

[e]Queensland University of Technology, GPO Box 2434, Brisbane, Qld 4001, Australia

Sara Marchetti: [a]POLARIS Research Centre, Department of Earth and Environmental Sciences, University of Milano-Bicocca, Piazza della Scienza 1, 20126 Milano, Italy. s.marchetti16@campus.unimib.it

* Corresponding author

Eleonora Longhin: [a]POLARIS Research Centre, Department of Earth and Environmental Sciences, University of Milano-Bicocca, Piazza della Scienza 1, 20126 Milano, Italy. eleonora.m.longhin@gmail.com

Rossella Bengalli: [a]POLARIS Research Centre, Department of Earth and Environmental Sciences, University of Milano-Bicocca, Piazza della Scienza 1, 20126 Milano, Italy. rossella.bengalli@unimib.it

Pasquale Avino: [b]DiAAA, University of Molise, via De Sanctis, 86100 Campobasso, Italy. p.avino@inail.it

Luca Stabile: [c]Department of Civil and Mechanical Engineering, University of Cassino and Southern Lazio, Via Di Biasio 43, 03043 Cassino (FR) Italy. l.stabile@unicas.it

Giorgio Buonanno: [c]Department of Civil and Mechanical Engineering, University of Cassino and Southern Lazio, Via Di Biasio 43, 03043 Cassino (FR) Italy. [4]University of Naples "Parthenope", Via Ammiraglio Ferdinando Acton, 38, 80133 Napoli, Italy. [5]Queensland University of Technology, GPO Box 2434, Brisbane, Qld 4001, Australia. buonanno@unicas.it

Anita Colombo: [a]POLARIS Research Centre, Department of Earth and Environmental Sciences, University of Milano-Bicocca, Piazza della Scienza 1, 20126 Milano, Italy. anita.colombo@unimib.it

Marina Camatini: [a]POLARIS Research Centre, Department of Earth and Environmental Sciences, University of Milano-Bicocca, Piazza della Scienza 1, 20126 Milano, Italy. marina.camatini@unimib.it

Paride Mantecca: [a]POLARIS Research Centre, Department of Earth and Environmental Sciences, University of Milano-Bicocca, Piazza della Scienza 1, 20126 Milano, Italy. paride.mantecca@unimib.it

Abstract

Biomass combustion significantly contributes to indoor and outdoor air pollution and to the adverse health effects observed in the exposed populations. Besides, the contribution to toxicity of the particles derived from combustion of different biomass sources (pellet, wood, charcoal), as well as their biological mode of action, are still poorly understood. In the present study, we investigate the toxicological properties of PM10 particles emitted indoor from a stove fueled with different biomasses.

PM10 was sampled by gravimetric methods and particles were chemically analyzed for Polycyclic Aromatic Hydrocarbons (PAHs) and elemental content. Human lung A549 cells were exposed for 24 hours to 1-10 μg/cm^2 PM and different biological endpoints were evaluated to comparatively estimate the cytotoxic, genotoxic and pro-inflammatory effects of the different PMs.

Pellet PM decreased cell viability, inducing necrosis, while charcoal and wood ones mainly induced apoptosis. Oxidative stress-related response and cytochrome P450 enzymes activation were observed after exposure to all the biomasses tested. Furthermore, after pellet exposure, DNA lesions and cell cycle arrest were also observed. The severe genotoxic and pro-necrotic effects observed after pellet exposure were likely the consequence of the high metal content. By administering the chelating agent TPEN, the genotoxic effects were indeed rescued. The higher content in PAHs measured in wood and charcoal PMs was likely

the reason of the enhanced expression of metabolizing and oxidative stress-related enzymes, like CYP1B1 and HO-1, and the consequent increase in apoptotic cell death.

These data suggest that combustion particles from different biomass sources may impact on lung cells according to different pathways, finally producing different toxicities. This is strictly related to the PM chemical composition, which reflects the quality of the combustion and the fuel in particular. Further studies are needed to clarify the role of particle dimension and the molecular mechanisms behind the harmful effects observed.

Keywords: biomass, PM10, air pollution, indoor, lung cells, cytotoxicity

Abbreviations

PM: Particulate matter; ROS: Reactive oxygen species; PAHs: polycyclic aromatic hydrocarbons; UFP: ultrafine particles; HO-1: hemeoxygenase 1; TPEN: N,N,N0,N0-tetrakis(2 pyridylmethyl)ethylenediamine; CDPs: combustion-derived particles; Zn: Zinc; Pb: lead; CYP1A1: Cytochrome P450, family 1, subfamily A, polypeptide 1; CYP1B1: Cytochrome P450 Family 1 Subfamily B Member 1; B[a]P: Benzo[a]pyrene; p-ATM: phosphoryled form of Ataxia Telangiectasia Mutated; γH2AX: Phosphorylated histone H2AX; GC/MS: gas chromatography-mass spectrometry; SIM: single ion monitoring; INAA: Instrumental Neutron Activation Analysis; TEM: transmission electron microscopy; SEM: scanning electron microscopy; RT: room temperature; PBS: Phosphate Buffered Saline; PI: Propidium Iodide; IL: Interleukin; O/N: overnight; TBS: Tris-Buffered Saline; TBS-T: TBS with 0.1% Tween20; SE: standard error of mean; OM: optical microscopy.

1. Introduction

The burning of biomass fuels for domestic heating is one of the most significant sources of particulate air pollutants during winter in the developed countries (Li et al., 2017; Secrest et al., 2016). Its role has increased in the last years as consequence of a general effort in improving the use of renewable energy sources and lower costs. Emissions from biomass combustion significantly contribute to the air pollution events and could cause severe health effects in adult and children (Samburova et al., 2016). Indoor air quality can differ with type of housing ventilation, energy technology (type of oven or stove used), environmental pollutant concentration and exposure time. Airborne and combustion particle exposure has been associated with increased lung cancer risk, exacerbation of respiratory diseases and cardiovascular impairment (Jalava et al., 2012; Sussan et al., 2014; Swiston et al., 2008). Furthermore, the International Agency for Research on Cancer (IARC), has classified biomass fuel combustion as probably carcinogenic to humans (Category 2A)("IARC Monographs on the Evaluation of Carcinogenic Risks to Humans," 2010).

Previous studies have investigated the toxicological effects of particles derived from biomass combustion in *in vitro* and *in vivo* systems, reporting ROS formation, activation of the response to polycyclic aromatic hydrocarbons (PAHs), DNA damage and cell death (Dilger et al., 2016; Happo et al., 2013; Muala et al., 2015). The results on inflammatory responses are controversial, since some papers report only minor activation (Kasurinen et al., 2017; Muala et al., 2015), while others highlight release of interleukins and activation of MAPK (Corsini et al., 2017; Uski et al., 2012). One reason of such differences might be related to the use of particles derived from different biomasses and combustion processes. In fact, particles collected from combustion of wood, animal dung, crop residues (Muala et al., 2015), coals (Capistrano et al., 2016), logs (Kasurinen et al., 2017), spring sandstorms or resuspension of local soil (Jin et al., 2016) are all referred as biomass. Therefore, the particle composition can be different depending on fuel type (Muala et al., 2015) and its

properties, including content of ash and moisture (Jin et al., 2016), chemical composition, combustion conditions (Lamberg et al., 2013) and combustion appliances used (Kocbach Bølling et al., 2009).

Recently, we reported low biological effects for biomass ultrafine particles (UFPs) produced by a modern boiler propelled with high quality certified pellet. Particle chemical characterization showed that this effect was associated to a low content of harmful compounds such as PAHs and metals (Longhin et al., 2016).

To date, the comprehension of the toxic effects induced by biomass particles emitted from different fuels is still poor. However, it is known that the physicochemical properties related to the content of transition metals and PAHs are associated to different cytotoxic properties, that could be responsible for the several adverse health effects caused by PM exposure (Jin et al., 2016; Yang et al., 2016).

This study intends to investigate how different fuels (i.e. pellet, charcoal and wood) used to propel the same stove (commonly used) may affect the properties of the emitted particles and their toxic potential.

Particulate matter (PM10) was sampled on filters by gravimetric technique and PAHs, metals content and particles morphology were investigated. The cytotoxic effect of PM10 was analyzed on the human alveolar A549 cells, that represent an extensively used model for inhalation toxicology purposes, and in particular for the PM cytotoxic effect (Chirino et al., 2017; Choi et al., 2016; Gualtieri et al., 2012; Kasurinen et al., 2017; Rossner et al., 2016). Cell viability, inflammatory response, antioxidant activity, xenobiotic metabolism activation, cell cycle alterations and DNA damage were evaluated.

Our data demonstrate that combustion particles deriving from different biomasses can activate different toxicological pathways, pointing out the role of the particle physico-chemical properties on the cytotoxic effects produced and the molecular mechanisms involved.

2. Materials and methods

2.1 Particles sampling

PMs were collected on filters through a gravimetric technique. The measurements were performed in a 20 m^3 room (with doors and windows closed) equipped with an open fireplace for 4 h. The fuel (pellet, charcoal or wood) was burnt in the open fireplace and continuously fed during the experiment. Three combustion tests were carried out for each fuel. Thus, PMs for biological investigation were sampled on Teflon filter, while particles for the chemical analysis were collected on laden quartz filters. PM10 concentrations were obtained after proper filter conditioning before and after particle samplings (Buonanno et al., 2011, 2009). The gravimetric sampler used was made up of a volumetric rotating pump Zambelli 6000 Plus (equipped with temperature and atmospheric pressure sensors to measure normalized sampling volume) and a Zambelli PM10 impactor (working at a nominal fixed flow rate of 2.3 m^3h^{-1} according to the EN 12341) to collect particles on low porosity filters for post-hoc analysis and PM10 mass concentration evaluation.

2.2 Particles characterization

2.2.1 Polycyclic aromatic hydrocarbons (PAHs)

The following PAHs were determined: acenaphthene, acenaphthylene, fluorene, phenanthrene, anthracene, fluoranthene, pyrene, benzo(a)anthracene, chrysene, benzo(b)fluoranthene, benzo(j)fluoranthene, benzo(k)fluoranthene, benzo(e)pyrene, benzo(a)pyrene, perylene, indeno(1,2,3,c,d)pyrene, dibenzo(a,h)anthracene and benzo(g,h,i)perylene. PAHs were quantified by gas chromatography-mass spectrometry (GC/MS) with an isotopic dilution method (Stabile et al., 2018). In particular, filters were spiked before the extraction with 5 ng of perdeuterated PAHs (L429-IS Internal Standard D-

IPA Stock Solution, Wellington Laboratories, Guelph, Canada); then the PAHs were Soxhlet-extracted in hexane for 24 h and the samples obtained were concentrated on a rotary evaporator (40 °C, 3.00×10^4 Pa) to 3-5 mL. Finally, the samples were automatically purified, by means of gel permeation chromatography, and concentrated, using an AccuPrep MPS & AccuVap Inline (J2 Scientific, Columbia, MO, USA).

GC/MS analysis was performed by an Ultra Trace gas chromatograph coupled with a TSQ mass spectrometer (Thermo Fischer Scientific, St Peters, MO, USA) used in single ion monitoring (SIM) mode. The column Meta-XLB (60 m length, 0.25 mm internal diameter, 0.25 μm film thickness; Teknokroma, Barcelona, Spain) was used for the separation, and He (99.9995% purity) was used as carrier gas. The temperatures for the injector, transfer line and ion source were set as 260 °C, 280 °C and 250 °C, respectively. The following oven temperature program was adopted: isothermal oven temperature of 60 °C for 1 min; thermal gradient of 20 °C min^{-1} up to 250 °C; isothermal oven temperature of 250 °C for 10 min; thermal gradient of 15 °C min^{-1} up to 300 °C; isothermal oven temperature of 300 °C for 15 min; thermal gradient of 5 °C min^{-1} up to 325 °C; isothermal oven temperature of 325 °C for 10 min. Each native PAH was quantified using its perdeuterated isotopologues as internal standard, except for acenaphthene (quantified using perdeuterated acenaphthylene), fluorene, anthracene (quantified using perdeuterated phenanthrene), pyrene (quantified using perdeuterated fluoranthene) and benzo(e)pyrene (quantified using perdeuterated benzo(a)pyrene). To calculate the extraction and purification recovery, 5 ng of recovery standard (L429-RS Recovery Standard D-IPA Stock Solution, Wellington Laboratories) were added before injection into the GC/MS. Recovery was calculated as the percentage ratio between the internal standard (added before the extraction) and the recovery standard (added before the injection in GC/MS). Perdeuterated acenaphthene was used to calculate the recovery of acenaphthylene and phenanthrene; perdeuterated pyrene was used to calculate the recovery of fluoranthene, benzo(a)anthracene and chrysene; perdeuterated

benzo(e)pyrene was used to calculate the recovery of benzo(b)fluoranthene, benzo(k)fluoranthene, benzo(a)pyrene, perylene, indeno(1,2,3,c,d)pyrene, dibenzo(a,h)anthracene and benzo(g,h,i)perylene.

2.2.2 Elements

The inorganic composition was investigated by a nuclear not-destructive technique: the Instrumental Neutron Activation Analysis (INAA). In particular, PMs (placed into the polyethylene tubes; Kartell, Milan, Italy) were irradiated by a Triga Mark II nuclear reactor of the ENEA-Casaccia Laboratories (1 MW power) (Capannesi et al., 2009). The irradiation was performed in the rotating rack, called Lazy Susan, which can give uniform neutron irradiation to the sample due to the continuous rotation. After neutron irradiation, the radionuclides begin to decay emitting γ-rays. The half-life time (t½), which is characteristic of nuclides produced, was adopted as criterion for element detection (Avino et al., 2000).

Basically, the γ-ray emission of nuclides with long t½ is negligible after short irradiation (Rabbit) (Avino et al., 2011). However, nuclides with short t½ were not detected because the sample was very active after the end of irradiation and the cooling time (3-5 days) is greater than the nuclide half-life; moreover, the nuclide activities with long half-lives hide the contribution (Avino et al., 2013, 2011). An 8 h long irradiation in the Lazy Susan was performed at a neutron flux of 2.6×10^{12} n s^{-1} cm^{-2}. At the end of irradiation, the samples were highly active and, according to the half-life of each elements, only few elements, such as As, Cd, Cr, Cu, Hg, Ni, Se and Zn could be analyzed, whereas Pb was separately analyzed by Inductively Coupled Plasma Atomic Emission Spectroscopy (ICP-AES). For the analysis, primary and secondary standards were used: primary standards (Carlo Erba, Milano, Italy) were Al, As, Br, Cl, Cu, I, Mg, Mn, Na, and V, whereas, as secondary standards, three reference materials (SRMs) such as SRM 2709 (S. Joaquim Soil) and SRM 98a (Plastic Clay) from the National Institute of Standards and Technology (NIST), and a SRM GRX-4

(Soil) from the US Geochemical Survey (USGS) were involved in this study. To guarantee the quality assurance and quality control (QA/QC) of the measurements performed, three SRMs along with the 8 primary standards were adopted: SRM 2709, SRM 98a, and SRM GRX-4. After irradiation, γ-ray spectrometry measurements of different durations were carried out using a Ge (HP) Canberra detector (Meriden, CT, USA) (full width at half maximum 1.68 keV at 1.332 keV) connected to a multichannel analyzer equipped with software packages (Canberra Genie 2k) for a γ-spectra analysis.

2.3 Particles extraction for biological investigations

Particles for *in vitro* exposures were obtain by extraction from Teflon filters according to a standardized procedure previously reported (Longhin et al., 2013). Briefly, filters from the same fuel were pooled in a glass vial and PM was extracted by an ultrasound bath (SONICA Soltec, Milan, Italy) by replicating four 20 min cycles using 2 mL of pure sterile water for each cycle. PM10 water suspensions were then collected in sterile tubes previously weighed, dried into a desiccator and the resulting pellet weighed to determine the mass of particles extracted. Finally, samples were stored at -20 °C until use. For biological investigations, particles were suspended in sterilized water to obtain aliquots at a final concentration of 2 μg/μL just before use. PM suspensions were sonicated for 30 secs just prior to cells exposure.

2.4 Morphological characterization of extracted particles

After extraction from the Teflon filters, a morphological characterization of the particles was performed by transmission electron microscopy (TEM) and scanning electron microscopy (SEM). Briefly, aliquots of 8 μL of sonicated particle suspensions at 25 μg/mL in pure water and 1% Isopropyl alcohol were respectively, pipetted on 200-mesh formvar-coated copper grids and aluminum stubs and dried at room temperature (RT). Samples were observed by

a Jeol JEM 1220 TEM, operating at 80kV, and a Tescan VEGA 5136XM, operating at 20kV. Images were digitally acquired and elaborated through dedicated softwares.

2.5 Cell culture and exposure

A549 cells, a human lung adenocarcinoma epithelial cell line, were obtained from the American Type Culture Collection (ATCC® CCL-185, American Type Culture Collection, Manassas, USA). Cells were cultured in OptiMEM I Reduced Serum Medium (Gibco, Life Technologies, Monza, Italy) supplemented with 10% heat-inactivated fetal bovine serum (FBS, Gibco) and Penicillin/Streptomycin (100 X, Euroclone, Pero, Italy) in a 5% CO_2 atmosphere at 37 °C.

For particle exposure, cells (passages 39 to 55) were seeded at a concentration of 2×10^4 cells/cm^2 (12-well plates) or $1.6x10^4$ cells/cm^2 (6-well plates), and grown up to 80% confluence for 24 h. At the optimal confluence, the culture medium was replaced with 1% FBS supplemented OptiMEM medium and cells exposed for 24 h at 37 °C to different doses (1, 2.5, 5, 7.5 and 10 µg/cm^2) for cellular metabolic activity evaluation and to 5 µg/cm^2 (50 µg/mL) PM10 for the following experiments. The same treatment was repeated for all the particles. Unexposed cells were used as control. Cells were exposed also to 14 µM benzo[a]pyrene (B[a]P, Sigma Aldrich, Saint Louis, MO, USA) for xenobiotic metabolism activation studies or 1.65 µM Etoposide (Sigma Aldrich) for DNA damage studies, as positive control (data not showed).

2.6 Cell viability

A549 cell viability was evaluated after 24 h of exposure to increasing PM10 concentrations (1-10 µg/cm^2) for each biomass particles by means of Alamar Blue assay. After exposure, the medium was removed, cells were rinsed twice with Phosphate Buffered Saline (PBS) and incubated for 3 h in 10% Alamar Blue (Invitrogen, Burlington, ON, Canada)

supplemented OptiMEM complete medium. The absorbance, proportional to cell metabolic activity, was assessed with a multiplate spectrophotometer reader (Tecan, Männedorf, Switzerland) at excitation and emission wavelengths of 570 and 630 nm respectively.

To provide additional data on biomass cytotoxicity, cell viability was evaluated also by fluorescence microscopy following cells staining with Hoechst 33342 (1 mg/mL) and Propidium Iodide (PI, 1 mg/mL). Briefly, after cells exposure to 5 μg/cm^2 PM, supernatants were harvested to recover floating cells, whereas attached cells were collected after trypsinization. Trypsinized and floating cells were then centrifuged at 1200 rpm, pooled, re-suspended in complete medium and stained 1:1 with Hoechst and PI for 20 min at RT in the dark. Cells were finally, centrifuged, re-suspended in FBS and smeared on a glass slide to quickly dry. Cell morphology was evaluated using a fluorescence microscope (Zeiss Axioplan). Cells were scored and classified on the different nuclear morphology as: viable (Hoechst positive and PI negative, with intact plasma membrane and without nuclear anomalies), necrotic (PI positive), apoptotic (bright Hoechst-stained with condensed and/or fragmented nuclei) and mitotic (Hoechst positive with chromosome condensation). At least 300 cells for each sample were scored. Additional cytofluorimetrical analyses were performed on cells stained with Annexin V/PI to assess the cell death modality (see Additional file 2).

2.7 Pro-inflammatory cytokines release

Intracellular and released protein levels of the pro-inflammatory cytokine Interleukin 6 (IL-6) and the chemokine IL-8 were measured by commercial enzyme-linked immunosorbent assay (ELISA) kits (IL-6, IL-8, Life Technologies). At the end of the exposure, cell supernatants were collected and centrifuged at 12000 rpm for 6 min at 4 °C to remove debris. The exposed cells were scraped and lysed on ice in RIPA buffer (150 mM NaCl, 1% TritonX-100, 0.5% sodium deoxycholate, 0.1% SDS, 50 mM Tris pH 8.0) and 0.1% of

proteases inhibitor, added just before use. The supernatants and cell lysates were stored at -80 °C until measurement. Cytokine analysis was performed according to the manufacturer's instructions. The absorbance of each sample was measured at 450 nm and the amount of proteins in pg/mL quantified by a plate reader (Multiplate Reader Ascent, Thermo Scientific, USA), based on a standard curve.

2.8 Protein extraction and immunoblotting

After exposure, cells for immunoblotting were rinsed twice, scraped and lysed on ice in RIPA buffer and 0.1% of proteases inhibitor, added just before use. Total cellular lysates were centrifuged at 12000 rpm for 15 min and the protein content evaluated by the bicinchoninic acid assay (Sigma Aldrich) according to the manufacturer's instructions. Equal amounts of proteins (30 µg) were loaded onto 12% SDS-PAGE gels, separated and transferred on nitrocellulose membranes. Equal loading was assessed by Ponceau S red staining of protein bands on nitrocellulose. Membranes were rinsed three times with water and Tris-Buffered Saline (TBS) with 0.1% Tween20 (TBS-T) and then, incubated for 1 h with Blocking buffer, TBS-T supplemented with 5% w/v bovine serum albumin (BSA; Sigma) or milk (Skim milk powder, Fluka, Sigma). Membranes were incubated overnight (O/N) at 4 °C with the specific primary antibody (HO-1 P249 Antibody, 1:1000, Cell Signaling Technology, Danvers, USA; Cytochrome P450 1A1 1:500 and CYP1B1, 1:500, Novus Biologicals, Littleton, CO, United States). The day after, membranes were rinsed three times with TBS-T and incubated with specific HRP-linked secondary antibodies in Blocking buffer for 1 h at RT (anti-rabbit IgG, 1:2000, Cell Signaling). Finally, membranes were rinsed as previously described, and exposed to Chemiluminescent Substrate (Euroclone). Monoclonal anti-β-Actin antibody (Cell Signaling, 1:1000) was used as loading control. Digital images were taken by a luminescence reader (Biospectrum-UVP, LLC, Upland, CA, United States) and densitometry analysis performed with dedicated software (Vision Works LS).

2.9 DNA damage analysis

Phosphorylated histone H2AX (γH2AX) and phosphoryled form of Ataxia Telangiectasia Mutated (p-ATM) were used as marker of DNA damage and analysis was performed by flow cytometry. After exposure, cells were trypsinized, washed and fixed with 1% paraformaldehyde in PBS at 4 °C for 15 min. Cells were gently re-suspended in 90% cold methanol and stored O/N at -80 °C prior to analysis. The samples were centrifuged at 1600 rpm for 6 min to discharge the methanol, washed once in PBS supplemented with 0.5% BSA and then, incubated with the specific antibody in PBS supplemented with 0.5% BSA and 0.2% Triton X-100. Alexa Fluor 488 conjugated γH2AX antibody (1:100, Cell Signaling) and a p-ATM mouse monoclonal antibody (1:100, Santa Cruz Biotechnology, Dallas, Texas, USA) were used. Cells stained for γH2AX were incubated for 4 h at RT, washed once in PBS 0.5% BSA, re-suspended in PBS and analyzed by the CytoFLEX 13/3. Cells stained for p-ATM were incubated with the primary antibody O/N at 4 °C. The day after, cells were washed once in PBS 0.5% BSA and incubated with the secondary antibody (Alexa Fluor 594 goat anti-mouse IgG, 1:500 dilution, Invitrogen/Molecular Probes, Eugene, Oregon, USA) in PBS 0.5% BSA, 0.2% Triton X-100 for 90 min at RT in the dark. Finally, cells were washed once, re-suspended in PBS and analyzed at the flow cytometer. The fluorescence of 10,000 events was detected using 525 (γH2AX) or 617 (p-ATM) nm band pass filter. The same cytometer setting was maintained for staining on independent experiment. Data were analyzed as mean percentage of positive cells for the staining.

Immunofluorescence analyses of p-ATM and γH2AX nuclear foci were also performed to confirm the cytofluorimetrical analysis (see Additional file 3).

2.10 Cell cycle analysis

The cell cycle progression of PM-treated cells was investigated after 24 h of exposure by DNA-staining. At the end of the exposure, cells were trypsinized, collected and pooled with the harvested medium. They were then, centrifuged at 1200 rpm for 6 min, fixed in 90% ethanol and stored at -20 °C until analysis. The cell cycle of unexposed control cells was analyzed too.

For the analysis, cells were centrifuged at 1600 rpm for 6 min to discharge the ethanol and resuspended in PBS and RNAse DNAse-free (1 mg/mL, Sigma-Aldrich, Italy) was added for 30 min at 37 °C. Finally, the fluorescent dye PI was added to stain DNA of cells for 7 min in the dark. Fluorescence was measured by flow cytometer (CytoFLEX 13/3) using 617 nm band pass filters and the analysis performed with the dedicated software (CytExpert software). A total of 10,000 events per sample were analyzed. We maintained the same cytometer setting for all the independent experiments performed. For the analysis, cells in different cell cycle phases were selected and analyzed as mean percentage of cells in each phase.

2.11 Treatment with metal chelator

The metal chelator TPEN (N,N,N0,N0-tetrakis(2-pyridylmethyl)ethylenediamine, Sigma) was used, since its high affinity for Zn^{2+}. TPEN was firstly dissolved in EtOH and used for incubating cells at the final concentration of 3 μM. This concentration has been selected after preliminary set up experiments. Particles were pre-incubated with TPEN for 1 h before the cells treatment and then added to cell medium. After 24 h exposure, cell cycle analysis was performed, as previously described (see par. 2.10).

2.12 Statistical Analysis

Mean and standard error of mean (SE) of at least three independent experiments, carried out following the same experimental conditions, are reported. Statistical analyses were

performed using GraphPad Prism 6 software, using One-way or Two-way ANOVA with Dunn's or Dunnett's post hoc multiple comparisons tests. Values of $p<0.05$ were considered statistically significant.

3. Results

3.1 Biomass PM10 chemico-physical characterization

The average mass fraction of PAHs emitted by pellet, charcoal and wood PMs are summarized in Table 1. A high PAH concentration was measured in PM10 emitted by charcoal and wood combustion processes with respect to pellet. BaP, recognized as the most cancerogenic PAH, was measured and its concentration resulted to be 4.03 ng_{BaP}/mg_{PM10}, 27.8 ng_{BaP}/mg_{PM10}, 62 ng_{BaP}/mg_{PM10} for pellet, charcoal and wood, respectively.

Polycyclic Aromatic Hydrocarbons (PAHs)	Pellet	Charcoal	Wood
Fluoranthene	22.7	173	124
Pyrene	25.3	197	219
Benzo[a]anthracene	5.1	38.8	54.4
Crysene	8.05	61.1	100
Benzo[b]fluoranthene	3.93	29.9	106
Benzo[k]fluoranthene	1.24	15	33.2
Benzo[e]pyrene	1.43	11.5	24.6
Benzo[a]pyrene	4.03	27.8	62
Perylene	0.76	7.44	13.3
Indeno[1.2.3.c.d]pyrene	1.74	12.4	49.1
Dibenzo[a.h]anthracene	0.69	4.55	1.94
Benzo[g.h.i]perylene	1.88	13.1	45.3
Total	76.85	591.6	832.8

Table 1. Average mass fractions of PAH on PM10 (ng/mg$_{PM10}$) emitted by pellet, charcoal and wood combustion processes.

Higher metal amounts were detected in PM10 emitted by pellet combustion compared to charcoal and wood, including As, Cd and Ni, which belong to Group 1 carcinogenic compounds ("IARC: Outdoor air pollution a leading environmental cause of cancer deaths," 2013), as summarized in Table 2. A negligible (lower than the detection limit) As amount was measured in charcoal and wood samples, whereas its concentration in PM10 emitted by pellet combustion was equal to 0.09 ng$_{As}$/µg$_{PM10}$. Ni and Cd concentration was 12.4 ng$_{Ni}$/µg$_{PM10}$ and 0.43 ng$_{Cd}$/µg$_{PM10}$, 5.7 ng$_{Ni}$/µg$_{PM10}$ and 0.17 ng$_{Cd}$/µg$_{PM10}$ and 7.2 ng$_{Ni}$/µg$_{PM10}$ and 0.24 ng$_{Cd}$/µg$_{PM10}$, for pellet, charcoal and wood combustion, respectively.

Metals	Pellet	Charcoal	Wood
As	0.09	<LOD	<LOD
Cd	0.43	0.17	0.24
Cr	6.2	5.5	5.1
Cu	3.5	2.8	4.1
Hg	7.9	2.3	3.1
Ni	12.4	5.7	7.2
Pb	19.3	2.9	0
Se	4.2	5.9	5.2
Zn	42.8	14.7	28.2
Total	96.82	39.97	53.14

Table 2. Average mass fractions of inorganic elements on PM10 (ng/µg$_{PM10}$) emitted by pellet, charcoal and wood combustion processes.

The particle morphology examined after filters extraction is reported in more detail in the additional Figure 1 [see Additional file 1]. It is evident that the particles deriving from the combustion of the different biomasses significantly differ in size and shape, with pellet PM

samples showing more particles with dimension in the ultrafine range. The PMs derived from charcoal and wood combustion appeared larger and with very irregular shapes (Figure 1).

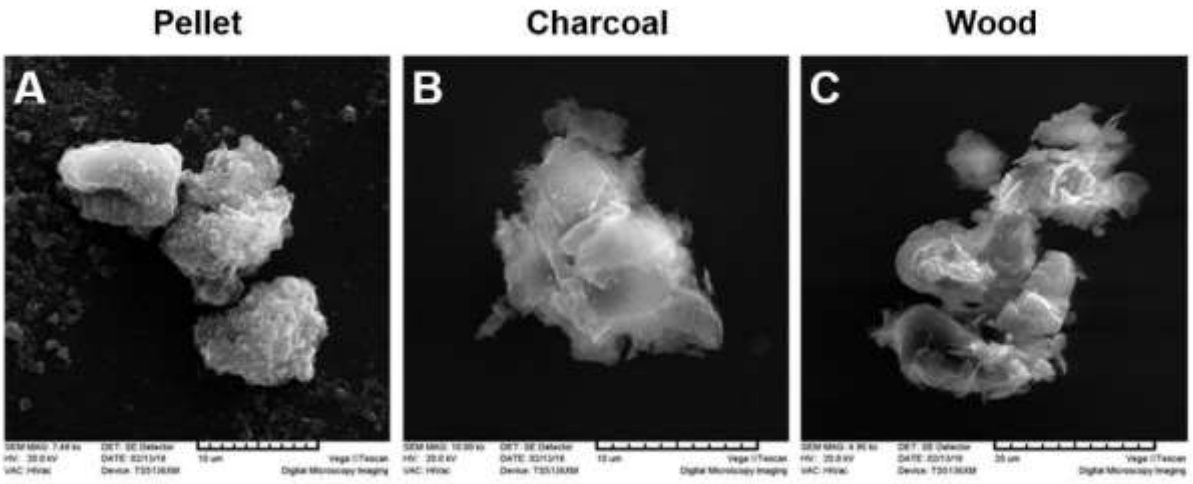

Figure 1 Morphological characterization of biomass PM10. Scanning Electron Microscopy (SEM) analysis on particles extracted from the sampling filters and suspended in sterile water: pellet **(A)**, charcoal **(B)**, and wood **(C)**.

3.2 Biomass PM10 biological effects

3.2.1 Cell viability

The cytotoxic effects were investigated by Alamar Blue assay (Figure 2) and Hoechst/PI staining (Figure 3) after 24 h exposure to PM10 from 1 μg/cm^2 to 10 μg/cm^2. A dose-dependent decrease in cell viability was observed (Figure 2), with significant differences in comparison to control starting from 5 μg/cm^2 for pellet PM and from 7.5 μg/cm^2 for wood (Two-way ANOVA; p<0.05). Cell viability was not affected after exposure to all the charcoal PM doses tested.

The dose of 5 μg/cm^2, showing low or no effects in the metabolic assay, was selected for the further experiments.

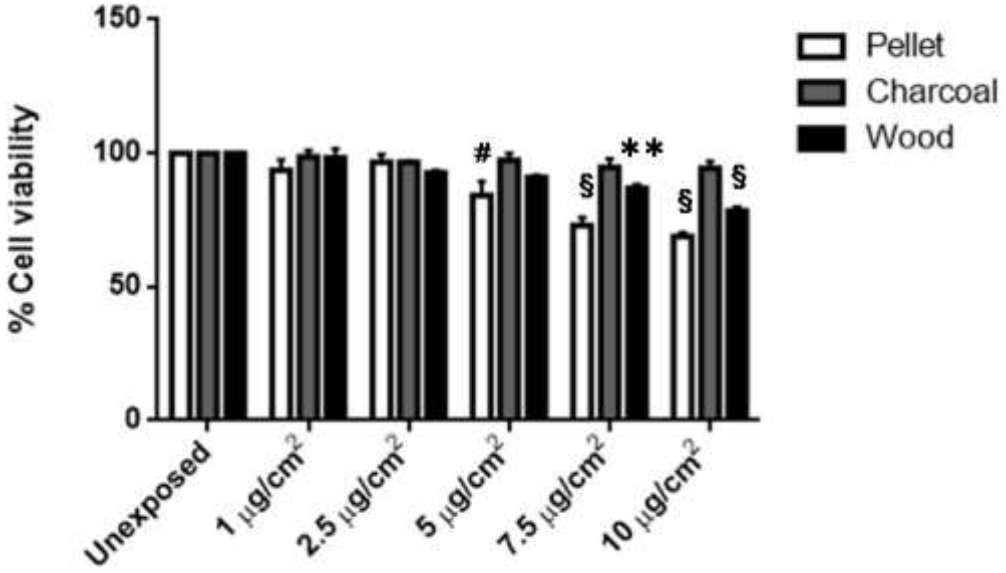

Figure 2 Cell viability assessed by Alamar Blue assay after 24 h exposure to increasing biomass PM concentrations: 0 (unexposed), 1, 2.5, 5, 7.5 and 10 µg/cm². Histograms represent the mean ± SE of at least three independent experiments. Statistical analysis was performed by Two-way ANOVA with Dunnett's multiple comparison test. $^{\S}p<0.0001$, $^{\#}p<0.001$ and $^{**}p<0.01$ *vs* control cells.

The differential cell count of the Hoechst/PI stained A549 cells, after exposure to 5 µg/cm² PMs for 24 h, suggested a significant decrease in the number of viable cells. In parallel a significant increase in necrotic cells (more than 14%) was induced by pellet, while charcoal and wood PMs significantly increased the number of apoptotic cells (more than 13% and 11% respectively) (Figure 3).

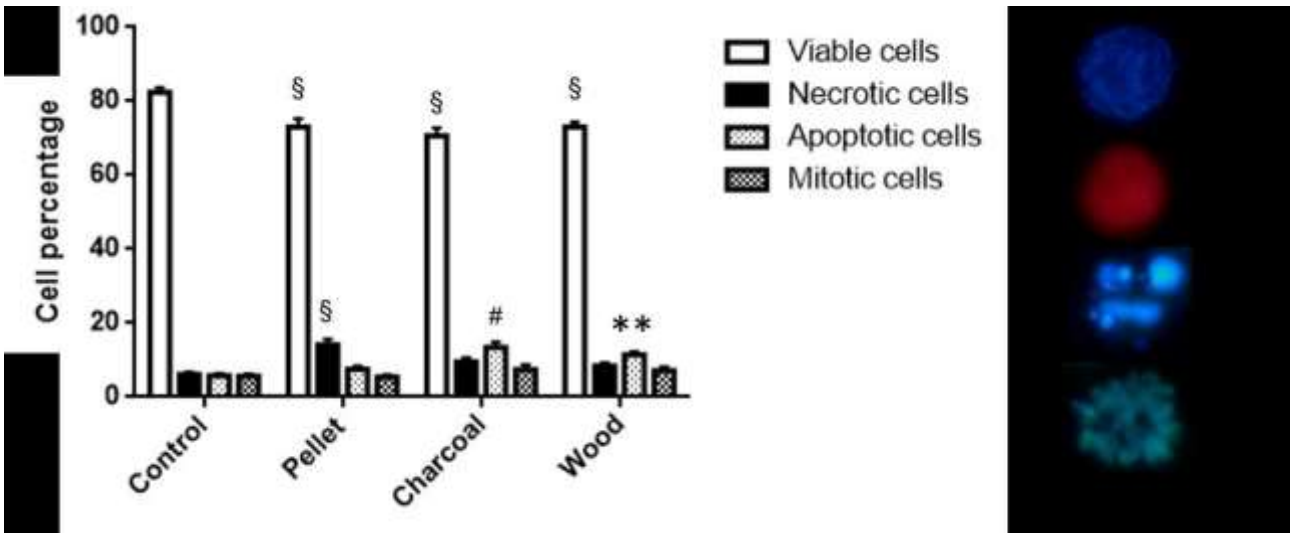

Figure 3 Cell viability assessed by Hoechst/PI staining after 24 h exposure to 5 µg/cm^2 biomass PMs

The differential cell count (viable, necrotic, apoptotic and mitotic cells) was based on the nuclei staining and morphology (see the right side of the panel). The data represent mean ± SE of three independent experiments. Statistical analysis was performed by Two-way ANOVA with Dunnett's multiple comparison test. $^{\S}p<0.0001$, $^{\#}p<0.001$ and $^{**}p<0.01$ *vs* control cells.

A more sensitive method was used to better discriminate the type of death mechanisms induced by biomass PMs [see Additional file 2]. Thanks to the cytofluorimetrical analysis of the Annexin V/PI staining, we were able to discriminate between necrosis and early or late apoptosis. The results confirmed necrosis as the main mechanism of cell death activated by pellet PM. As shown in the Additional Figure 2, charcoal and wood PMs, activated also the apoptotic process, with a slight increased number of cells in early and late apoptosis compared to control and pellet exposed cells.

3.2.2 Synthesis and release of pro-inflammatory cytokines

To investigate the inflammatory response, the release of two key pro-inflammatory mediators, IL-6 and IL-8, was measured after A549 cells exposure to 5 µg/cm^2 PM10 for 24 h. No significant increase in IL-6 and IL-8 secretion was obtained after exposure to all the biomass PMs (Figure 4A and C). Only a slight increase of IL-6 was observed in pellet-

exposed cells (Figure 4A). The intracellular levels of the proteins were also analyzed (Figure 4B and D). IL-8 expression significantly increased in pellet-exposed cells (One-way ANOVA; $p<0.05$), while charcoal and wood did not affect IL-8 levels. IL-6 intracellular concentration is higher in the cells exposed to all PMs. Anyway, such increase was not statistically significant (Figure 4B).

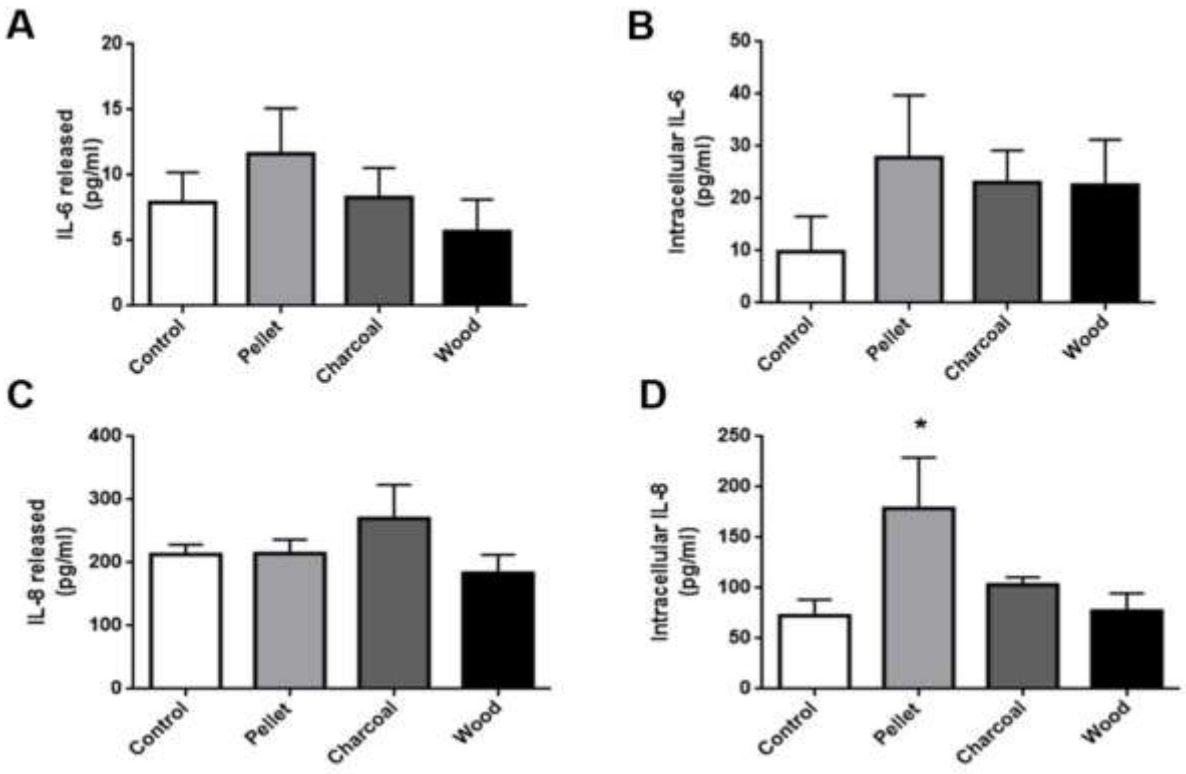

Figure 4 Pro-inflammatory effects induced by biomass PMs after exposure to 5 µg/cm^2. A) IL-6 secretion. **B)** Intracellular level of IL-6. **C)** IL-8 secretion. **D)** Intracellular level of IL-8. Results are expressed as mean ± SE of five independent experiments. Statistical analysis was performed by One-way ANOVA with Dunnett's multiple comparison test. *$p<0.05$ *vs* control cells.

3.2.3 Antioxidant response

The activation of the anti-oxidant response was also evaluated. The expression of hemeoxygenase 1 protein (HO-1) was assessed by Western Blot. As showed in Figure 5, a

statistically significant increase in HO-1 expression was observed after exposure to all the three PMs, with wood particles inducing the highest effect.

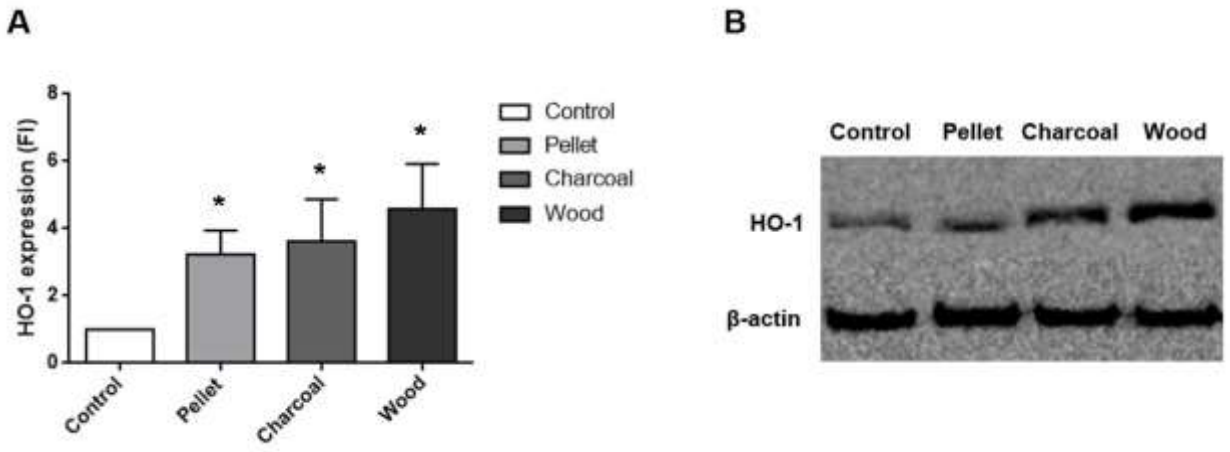

Figure 5 Expression of the oxidative stress marker HO-1. A) Protein analysis after exposure to biomass PMs. Data are presented as mean ± SE of five independent experiments. Statistical analysis was performed by One-way ANOVA with Dunn's multiple comparison test. *p<0.05 *vs* control cells. **B)** Representative immunoblotting images displaying HO-1 expressed from A549 cells exposed for 24 h to 5 μg/cm^2. β-Actin was used as control.

3.2.4 Xenobiotic metabolism activation

The expression of the enzymes CYP1A1 and CYP1B1, involved in PAHs metabolism, was analyzed. As shown in Figure 6A, CYP1A1 protein level was not significantly increased by biomass PMs exposure at the dose and time point investigated. On the contrary, positive results were obtained for CYP1B1, with a mild increase of the protein level in cells exposed to pellet, a strong, although not statistically significant, increase in cells exposed to charcoal, and a definite statistically significant increment in cells exposed to wood PM (Figure 6B).

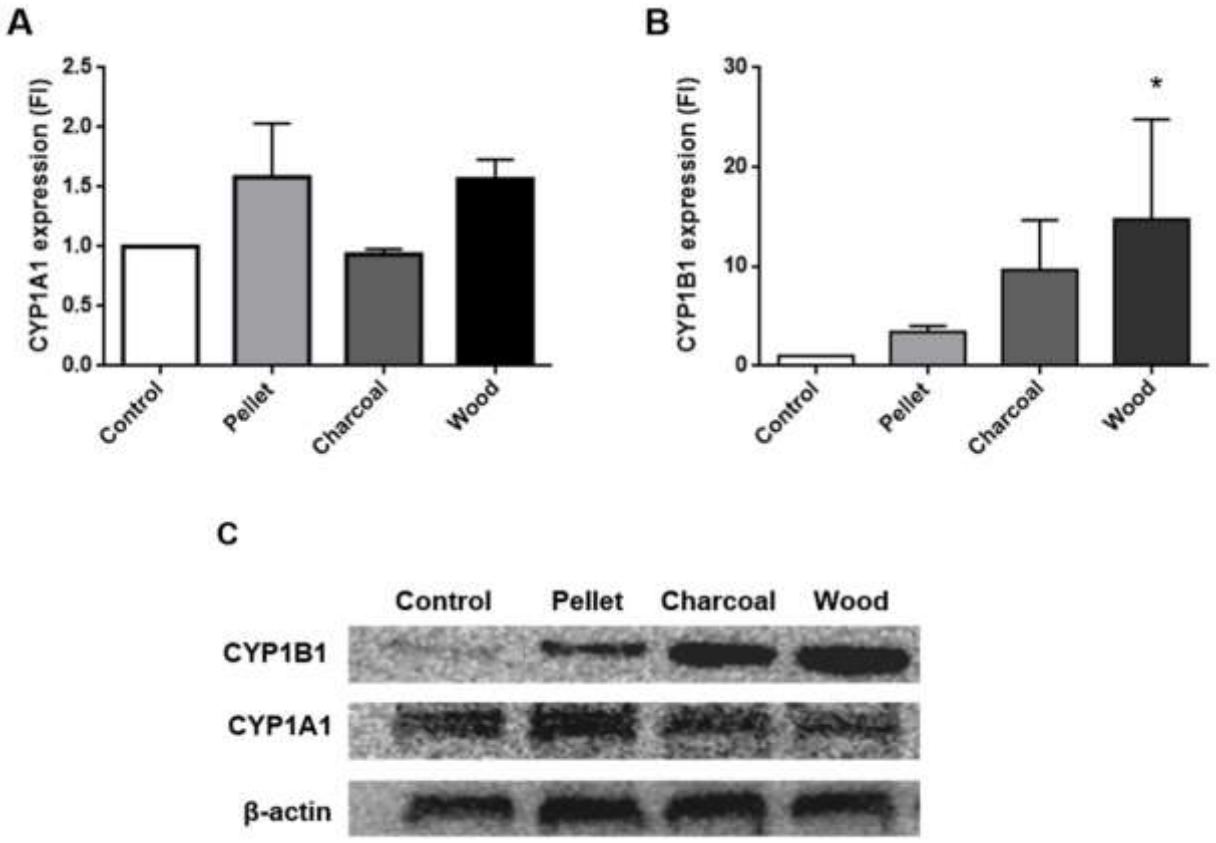

Figure 6 Activation of PAH-metabolizing enzymes cytochromes P450 (CYPs). A, B) Histograms represent CYP1A1 and CYP1B1 expression respectively. Data are presented as mean ± SE of three independent experiments. Statistical analysis was performed by One-way ANOVA with Dunn's multiple comparison test. *p<0.05 *vs* control cells. **C)** Representative immunoblotting images displaying CYP1A1 and CYP1B1 expressed from A549 cells exposed for 24 h to 5 μg/cm^2. All the data were normalized to β-actin.

3.2.5 DNA damage

DNA strand breaks were evaluated by the quantification of the activated form of ATM (p-ATM). To determine if p-ATM activation is followed by H2AX phosphorylation, which reflects the activation of DNA repair mechanisms, cells were also stained and scored for γH2AX. As shown in Figure 7, only the exposure to pellet PM led to a significant augmented expression of p-ATM compared to the control cells, but it is associated only to a slight activation of γH2AX. It is noteworthy that A549 cells showed high background levels of γH2AX, possibly masking eventual increases induced by PM exposure (Figure 7B). A representative

immunofluorescence image showing the foci of DNA damage (p-ATM) after the exposure to Pellet PM is reported in the additional Figure 3 [see Additional file 3].

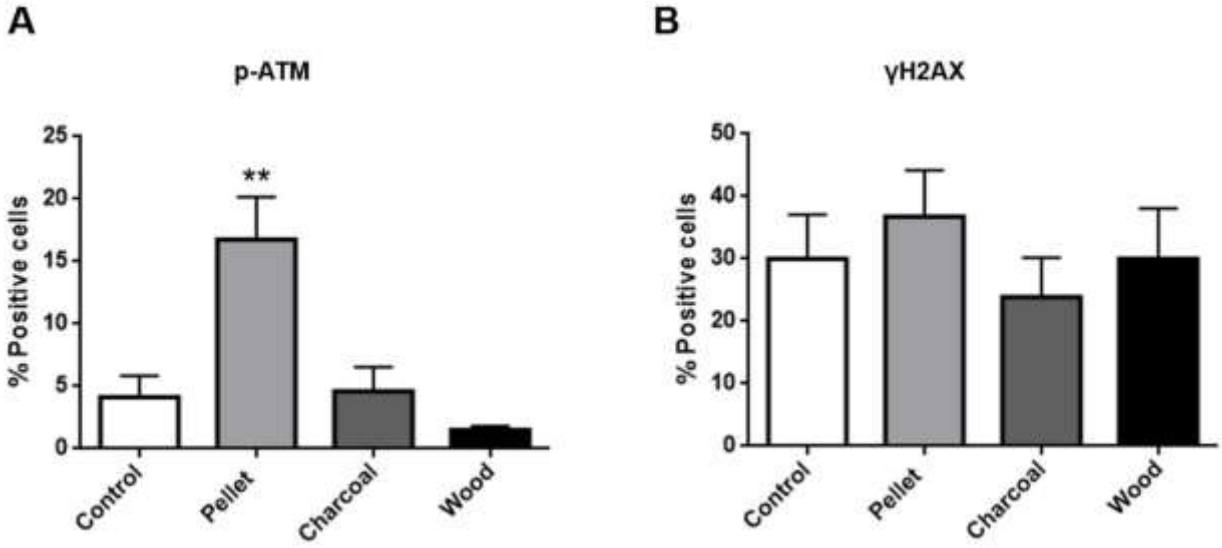

Figure 7 Induction of ATM and H2AX phosphorylation in A549 cells following exposure to biomass PMs. The histograms show the percentage of positive cells for p-ATM expression **(A)** and for γH2AX expression **(B)**. Data are presented as mean ± SE of three independent experiments. Statistical analysis was performed by One-way ANOVA with Dunnett's multiple comparison test. ***p*<0.01 *vs* control cells.

3.2.6 Cell cycle analysis

A549 cells exposed to 5 μg/cm^2 of charcoal and wood PMs did not show cell cycle alterations, while those exposed to pellet PM did (Figure 8A). Pellet-exposed cells presented a significant increase in G0-G1 phase (from 62.27% of control cells to 76.47%), with a parallel decrease in S and G2-M phases. These results confirm the genotoxic effect, already evidenced by DNA repair system activation, specifically produced by pellet PM.

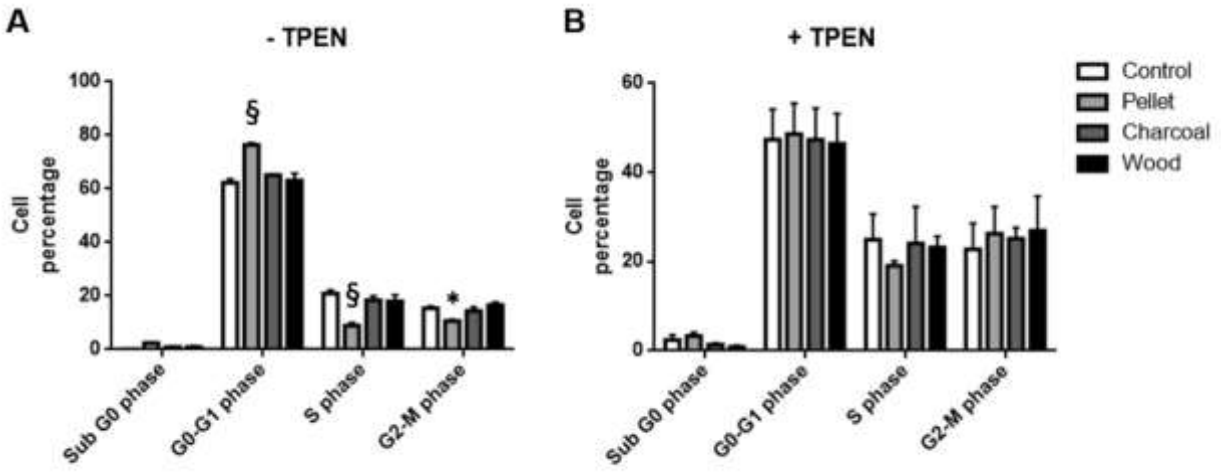

Figure 8 Cell percentage in each phase of the cycle (SubG0, G1, S, G2/M) after exposure to 5 µg/cm² biomass PMs pre-incubated (B) or not (A) with TPEN. A) Cells exposed to PMs. **B)** Cells exposed to PMs pre-incubated with TPEN. Data are presented as mean ± SE of four independent experiments. Statistical analysis was performed by Two-Way ANOVA with Dunnett's multiple comparison test. §p<0.0001 and *p<0.05 *vs* control cells.

The metal chelator TPEN (N,N,N0,N0-tetrakis(2-pyridylmethyl)ethylenediamine) was used to investigate the role of Zinc in the pellet-induced cell cycle alterations. TPEN per se had a slight but not significant effect on the cell cycle, but it was able to completely rescue the alterations induced by pellet PM (Figure 8B).

4. Discussion

There is today a general awareness that the atmospheric PM-induced biological effects could depend on the particle physico-chemical composition and on the sources of emissions, but still much remains to be explained about the role of specific combustion processes and fuels in determining the toxicity of the emitted particles. In this perspective, more research is needed to understand the toxicological properties of combustion-derived

particles (CDPs), the specific biological mechanism of action and their role in the adverse health effects observed in the exposed populations.

In the present work, we compared the chemical composition and the biological effects of three different biomass CDPs, sampled indoor as PM10 during combustion of pellet, charcoal and wood, using the same stove. PM10s were analyzed for PAHs and metals content and their cytotoxic, pro-inflammatory and genotoxic effects were evaluated *in vitro* on human lung A549 cells.

Charcoal and wood PMs, mainly induced the xenobiotic response enzymes activation and cell apoptosis. Interestingly, pellet particles displayed a different toxicological mechanism, inducing a mild inflammatory response, DNA damage and cell cycle arrest in G1 phase and the consequent cell death by necrosis. Such a difference in the toxicological profiles was likely dependent on the different relative abundances of PAHs and heavy and transition metals observed in the PMs. Indeed, pellet PM contained higher amounts of metals compared to charcoal and wood that, on the contrary, resulted enriched in PAHs.

Among metals, Zinc (Zn) was the most abundant in all samples, but with a concentration in pellet particles 1.5- and 3-fold higher than in wood and charcoal, respectively. Also lead (Pb) concentration presented great differences among the particles, being 6-fold higher in pellet than in charcoal, while it was not detected in wood particles. A higher cytotoxicity of Zn-enriched biomass particles, compared to particles with lower Zn content, was already suggested (Uski et al., 2015), and ZnO particles were shown to induce cell apoptosis or necrosis, according to the cell exposure to lower or higher doses respectively (Zhang et al., 2012). A correlation between cytotoxicity and Pb content in airborne PM was also reported, so as for other metals, such as Cd, As, Cr, and Cu (Michael et al., 2013; Perrone et al., 2010; Van Den Heuvel et al., 2016), and a definitely higher concentration of this metal in pellet PM in respect to wood and charcoal ones.

On the contrary, charcoal and wood particles displayed a PAH content approximatively 10-fold higher than pellet ones. Such lower metal content, together with the relatively high PAH content may be responsible of the reduced cytotoxicity and the slightly increased apoptotic event in charcoal and wood exposed cells. This is also in agreement with previous studies, showing that high concentrations of PAHs in urban PM are strongly associated with apoptosis (Uski et al., 2014; Yang et al., 2016), and that PAH-coated carbon particles are able to induce apoptosis in tracheal epithelial cells, while pristine particles are not (Lindner et al., 2017). All together, these observations suggest that the particle-adsorbed chemicals might activate different cell death mechanisms.

The activation of the inflammatory pathway was also investigated as important cell response to biomass PM, possibly involved in necrotic and/or apoptotic processes (Nemmar et al., 2013; Wallach et al., 2013). The levels of IL-6 and IL-8, two main pro-inflammatory mediators, were measured in both the intracellular and the extracellular compartments. At the subtoxic dose tested, no significant responses were observed, except for a slight increase in the intracellular level of IL-6 after exposure to all PMs and a statistically significant increase in the intracellular IL-8 in pellet PM-exposed cells (Figure 4). In literature, the results concerning the biomass particles inflammatory potential are controversial. In A549 cells exposed to diverse wood/biomass particles, low pro-inflammatory cytokines release has been generally reported (Corsini et al., 2017; Danielsen et al., 2011; Dilger et al., 2016). Also in RAW264.7 macrophages wood smoke particles were found to induce cell death with only minor inflammatory response (Muala et al., 2015). In a previous study on ambient PM, we observed that IL-8 response was induced by the fine PM fraction (PM1), manly as a consequence of the metal content - As and Zn in particular - as demonstrated by PCA analysis (Perrone et al., 2010). Metals in general are known to induce inflammatory responses, thus the increased IL-8 expression in cells exposed to pellet PM may be related to the higher metal content displayed. The differences between IL-8 intracellular and

extracellular expression could be due to an inhibitory effect of the PM on the secretion of IL-8 soluble form. A mismatch between IL-8 gene expression and lack of augmented extracellular release has previously been reported following exposure to urban PM2.5 (Alfaro-Moreno et al., 2009; Kocbach et al., 2008). This IL-8 suppression could be due to PAHs or other chemicals present in the PM, as reported also by previous studies (Fuentes-Mattei et al., 2010; Totlandsdal et al., 2014).

Since the biomass PMs, especially charcoal and wood ones, are enriched in PAHs, we evaluated the activation of two main enzymes of the cytochrome P450 superfamily, CYP1A1 and CYP1B1, that are involved in the xenobiotic metabolism response (Dilger et al., 2016; Rossner et al., 2016). We found a significant induction of CYP1B1 in wood CDPs-exposed cells, in agreement with the highest PAH content. Pellet CDPs did not induce a significant activation of CYP enzymes, accordingly to the lower PAH levels. Although it may seem unexpected, the overall lower induction of CYP1A1 is in agreement with previous studies, in which CYP1B1 resulted more responsiveness than CYP1A1 in A549 cells exposed to urban PM2.5 and Benzo[a]pyrene (B[a]P) (Genies et al., 2013; Gualtieri et al., 2012). Furthermore, according to Genies (2016), A549 response to PAHs could be influenced by their behavior in a mixture of compounds. Individual PAHs indeed, upregulate in different ways the two enzymes, but their toxic properties could be inhibited or enhanced when they are combined. Since PM is a complex mixture of PAHs, the differences in the concentration of individual PAHs could be therefore responsible for the different responses observed after exposure to biomass PMs. Interestingly, in previous papers the induction of CYP1B1, and not of CYP1A1, was observed after exposure to urban PM2.5 and PM10 in both *in vitro* (A549 cells) and *in vivo* systems (Gualtieri et al., 2012; Farina et al., 2013). It may be supposed that specific PAHs and/or the presence of other molecules (e.g. TCDD) may contribute in the expression of such enzyme. Moreover, according to Hukkanen and colleagues (2000) the expression of CYP1B1 by TCDD (2,3,7,8- tetrachlorodibenzo-p-dioxin) is less

dependent on AHR. Interestingly it has also been reported that CYP1B1 mRNA is the most sensitive target across different cell models compared to CYP1A1 and other three less frequently used AhR target genes (TIPARP, AHRR, ALDH3A1), while CYP1A1 mRNA induction is strictly AhR-dependent (Strapáčová et al., 2018).

Oxidative stress is a main mechanism of PM-mediated cytotoxicity, able to induce cellular damage by targeting several cellular components, including proteins, lipids and nucleic acids. Both PAHs and metals are able to induce ROS production (Crobeddu et al., 2017; Yang et al., 2016), and in response to oxidative stress cells might react modulating the expression of heme oxygenase 1 (HO-1), one of the key enzyme involved in the anti-oxidant activity (Dilger et al., 2016). Not surprisingly, our results showed that all biomass PMs were able to activate the anti-oxidant response, inducing a statistical significant increase of the HO-1 expression, independently from their chemical compositions.

Since the PM-induced oxidative stress may result in genotoxic effects, the presence of DNA lesions was then evaluated by quantifying the expression of p-ATM and γH2AX. One of the main signaling pathways that help cells to respond to DNA insults involves the ataxia-telangiectasia mutated (ATM) kinase, which is activated by double strand breaks (DSBs) induced by radiations, oxidative stress and genotoxins (Maréchal and Zou, 2013; Smith et al., 2010). ATM activation triggers a cascade of events that lead to the phosphorylation of different substrates, including H2AX, BRCA1, Chk1/2 and p53, involved in DNA repair, cell-cycle arrest or apoptosis processes. The key event deriving from ATM activation is the phosphorylation of the histone H2AX (γH2AX), that is required for the activation of DNA repair proteins to the damage site (Maréchal and Zou, 2013; Sànchez-Pérez et al., 2009). Although DNA primary lesions generally occur after 6 h of exposure, our results indicate that also after 24 h it is possible to observe genotoxic lesions. Similar evidences have been observed also in other previous works, even at reduced concentrations compared to the one selected for our research (Gualtieri et al., 2011; Longhin et al., 2013; Marabini et al., 2017).

Such differences in the timing of the response to DNA damage may be due to the delayed bioavailability of PAHs carried out by the CDPs. Since PAHs are adsorbed onto the carbonaceous particles, their effects on the cell metabolic response can take place only after the endocytosis and the consequent availability of the xenobiotics at the level of the smooth endoplasmic reticulum (SER), where the metabolism enzymatic systems are located.

Our results indicate an increased expression of p-ATM and a slight modulation of γH2AX only after pellet exposure, suggestive of DNA lesions, followed by the tentative to activate the DNA repairing machinery. This partial activation might be responsible of the significant cell cycle arrest in G1 phase and cell death by necrosis induced by pellet CDPs.

The reason why no DNA damages were revealed after wood and charcoal exposure may reside in the fact that ROS generation by PAHs involves their conversion into quinones, which are able to generate bulky DNA adducts, not recognized by ATM. On the contrary, metals, generating hydroxyl radicals, could trigger the accumulation of DNA strand breaks that finally activate ATM (Henkler et al., 2010; Rudolf and Cervinka, 2011).

The cell-signaling pathway activated in presence of oxidative DNA damage has been suggested as one of the mechanisms behind cell cycle arrest. DNA damage indeed, activates different checkpoints, finally inhibiting cell cycle progression. Besides, the activated checkpoint may depend on the type of damage (Cuadrado et al., 2006; Gualtieri et al., 2011; Liang et al., 2009). In the present study, only the samples exposed to pellet CDPs showed a significant cell cycle modification, with many cells blocked in G1 phase. This is in accordance with previous data, in which the arrest in G0 checkpoint is reported to be associated to DNA damage and increased cellular levels of p53 (Liang et al., 2009; Kastan et al., 1991). Other studies demonstrated the PM-induced arrest of cell cycle in G1 (Reyes-Zárate et al., 2016; Zhang et al., 2007) and in G2/M phase (Longhin et al., 2013), as a function of the variable chemical composition. The amount and type of PAHs was probably the main responsible of to the mitotic arrest, while the higher amount of metals in

pellet CDPs could be responsible for the arrest in G1 phase, as already suggested (Steenhof et al., 2011). It was reasonable to suspect that Zinc, present in a very high concentration in pellet PM, contributes significantly to the cytotoxic and genotoxic effects of this PM type, even considering the significant cell cycle rescue achieved after incubation with the Zinc chelator probe, TPEN (Figure 8B). Zinc, and in general transition metals, are known to significantly induce oxidative DNA damage through Fenton reaction-generated ROS, with the consequent accumulation of DNA lesions preventing cells to enter S phase. From the literature, it is known that PM samples containing high Zn concentrations display elevated toxic properties (Torvela et al., 2014; Uski et al., 2015) and that Zn ions and Zn nanoparticles produce significant DNA damage (Pati et al., 2016; Rudolf and Cervinka, 2011). Of course, the very high content of other heavy metals, e.g. Pb and Mercury (Hg), does not allow us to exclude an involvement also of these elements in the enhanced toxicity observed after treatment with pellet CDPs.

In a recent publication we reported that UFPs obtained from the combustion of high- quality certified pellet in a modern automatic 25 kW boiler did not induce significant toxicity in human bronchial cells at concentrations similar to those used in the present study, contrary to diesel exhaust particles, which displayed cytotoxic and genotoxic effects (Longhin et al., 2016). These results clearly point out that the quality of the biomass used and the combustion technology may drastically influence the quality of the emitted particles, with the size and the relative abundance of metals and PAHs as the main physico-chemical variables affected.

5. Conclusions

According to the main evidences of the present study, the physico-chemical properties of the biomass CDPs, reflecting the efficiency of the combustion systems and the biomass fuel

quality, do not only influences the acute toxicity, but even the cellular mechanism of action, pointing out the need of further exploring the adverse outcome pathways. In this regard, recently the Air Liquid Interface (ALI) exposure systems received attention as an alternative method to the submerged system in studying the biological effects of ultrafine particles (Loxham et al., 2015) and nanoparticles (Kim et al., 2013). Nevertheless, the widespread adoption of ALI systems is still limited for PM by the minimal efficiency of particles deposition and by the complex strategy needed to characterize the composition of the particles delivered to the cells (Kim et al., 2013). Besides, studies on the comparative biological effects of the UFPs deriving from controlled combustion processes, using 3D lung *in vitro* systems exposed at the ALI, will be of high relevance to depict the hazardous behavior of the different biomass CDPs.

In conclusion, different adverse biological outcomes can result from the exposure to biomass CDPs and the present data confirm that the amount of metals is crucial in inducing acute effects related to cytoxicity and genotoxicity, while PAHs are responsible for the induction of the xenobiotic metabolizing systems and the oxidative stress cell responses. Since these variable effects induced by solid biomass CDPs, the chemical composition of particles and their toxicological profiles should be known in order to suggest efficient strategies for the prevention of the adverse health effects in indoor exposure, but also for the management of outdoor air quality at local level.

Further investigations are of course needed to better define the molecular mechanisms of action but, at the same time, more stringent regulations are required to guarantee high quality biomass fuels and safer combustion technologies.

Acknowledgments

SM performed the experiments and manuscript writing. EL performed the particles extraction, supervised the flow cytometry analysis, interpreted the results and contributed to writing the manuscript. RB performed the TPEN analysis, interpreted the results and helped with the writing of the manuscript. PA conducted the chemical analysis. LS conducted the PM sampling and helped with the writing of the manuscript. GB defined the experimental plan, conducted the PM sampling and helped with the writing of the manuscript. AC helped with the particle morphological characterization, supervised all the experiments and contributed to writing the manuscript. MC defined the experimental plan, supervised all the experiments and contributed to writing the manuscript. PM performed the morphological analysis, supervised all the experiments and contributed to writing the manuscript. All authors read and approved the final manuscript.

Funding

This study has been supported by the grants of the Cariplo Foundation to MC (proj. ID 2013-1038) and the Italian Ministry of Foreign Affairs and International Cooperation to PM (proj. ID PGR00786).

Conflicts of interest

The authors declare no conflicts of interest.

References

Alfaro-Moreno, E., Torres, V., Miranda, J., Martínez, L., García-Cuellar, C., Nawrot, T.S.,

Vanaudenaerde, B., Hoet, P., Ramírez-López, P., Rosas, I., Nemery, B., Osornio-Vargas, A.R., 2009. Induction of IL-6 and inhibition of IL-8 secretion in the human airway cell line Calu-3 by urban particulate matter collected with a modified method of PM sampling. Environmental Research 109, 528–535. doi:10.1016/j.envres.2009.02.010

Avino, P., Capannesi, G., Renzi, L., Rosada, A., 2013. Instrumental neutron activation analysis and statistical approach for determining baseline values of essential and toxic elements in hairs of high school students. Ecotoxicology and Environmental Safety 92, 206–214. doi:10.1016/j.ecoenv.2013.01.029

Avino, P., Capannesi, G., Rosada, A., 2011. Ultra-trace nutritional and toxicological elements in Rome and Florence drinking waters determined by Instrumental Neutron Activation Analysis. Microchemical Journal 97, 144–153. doi:10.1016/j.microc.2010.08.007

Avino, P., Carconi, P.L., Lepore, L., Moauro, A., 2000. Nutritional and environmental properties of algal products used in healthy diet by INAA and ICP-AES. Journal of Radioanalytical and Nuclear Chemistry. doi:10.1023/A:1006721811478

Buonanno, G., Dell'Isola, M., Stabile, L., Viola, A., 2011. Critical aspects of the uncertainty budget in the gravimetric PM measurements. Measurement: Journal of the International Measurement Confederation 44, 139–147. doi:10.1016/j.measurement.2010.09.037

Buonanno, G., Dell'Isola, M., Stabile, L., Viola, A., 2009. Uncertainty budget of the SMPS-APS system in the measurement of PM 1, PM2.5, and PM10. Aerosol Science and Technology 43, 1130–1141. doi:10.1080/02786820903204078

Capannesi, G., Rosada, A., Avino, P., 2009. Elemental characterization of impurities at trace and ultra-trace levels in metallurgical lead samples by INAA. Microchemical Journal 93, 188–194. doi:10.1016/j.microc.2009.07.004

Capistrano, S.J., Zakarya, R., Chen, H., Oliver, B.G., 2016. Biomass smoke exposure enhances rhinovirus-induced inflammation in primary lung fibroblasts. International Journal of Molecular Sciences 17. doi:10.3390/ijms17091403

Chirino, Y.I., García-Cuellar, C.M., García-García, C., Soto-Reyes, E., Osornio-Vargas, Á.R., Herrera, L.A., López-Saavedra, A., Miranda, J., Quintana-Belmares, R., Pérez, I.R., Sánchez-Pérez, Y., 2017. Airborne particulate matter in vitro exposure induces cytoskeleton remodeling through activation of the ROCK-MYPT1-MLC pathway in A549 epithelial lung cells. Toxicology Letters 272, 29–37. doi:10.1016/j.toxlet.2017.03.002

Choi, Y., Park, K., Kim, I., Kim, S.D., 2016. Combined toxic effect of airborne heavy metals on human lung cell line A549. Environmental Geochemistry and Health. doi:10.1007/s10653-016-9901-6

Corsini, E., Ozgen, S., Papale, A., Galbiati, V., Lonati, G., Fermo, P., Corbella, L., Valli, G., Bernardoni, V., Dell'Acqua, M., Becagli, S., Caruso, D., Vecchi, R., Galli, C.L., Marinovich, M., 2017. Insights on wood combustion generated proinflammatory ultrafine particles (UFP). Toxicology Letters 266, 74–84. doi:10.1016/j.toxlet.2016.12.005

Crobeddu, B., Aragao-Santiago, L., Bui, L.C., Boland, S., Baeza Squiban, A., 2017. Oxidative potential of particulate matter 2.5 as predictive indicator of cellular stress. Environmental Pollution 230, 125–133. doi:10.1016/j.envpol.2017.06.051

Cuadrado, M., Martinez-Pastor, B., Murga, M., Toledo, L.I., Gutierrez-Martinez, P., Lopez, E., Fernandez-Capetillo, O., 2006. ATM regulates ATR chromatin loading in response to DNA double-strand breaks. The Journal of experimental medicine 203, 297–303. doi:10.1084/jem.20051923

Danielsen, P.H., Møller, P., Jensen, K.A., Sharma, A.K., Wallin, H., Bossi, R., Autrup, H., Mølhave, L., Ravanat, J.-L., Briedé, J.J., de Kok, T.M., Loft, S., 2011. Oxidative

stress, DNA damage, and inflammation induced by ambient air and wood smoke particulate matter in human A549 and THP-1 cell lines. Chemical research in toxicology 24, 168–84.

Dilger, M., Orasche, J., Zimmermann, R., Paur, H.-R., Diabaté, S., Weiss, C., 2016. Toxicity of wood smoke particles in human A549 lung epithelial cells: the role of PAHs, soot and zinc. Archives of Toxicology 90, 3029–3044. doi:10.1007/s00204-016-1659-1

Farina, F., Sancini, G., Battaglia, C., Tinaglia, V., Mantecca, P., Camatini, M., Palestini, P., 2013. Milano Summer Particulate Matter (PM10) Triggers Lung Inflammation and Extra Pulmonary Adverse Events in Mice. PLoS ONE 8. doi:10.1371/journal.pone.0056636

Fuentes-Mattei, E., Rivera, E., Gioda, A., Sanchez-Rivera, D., Roman-Velazquez, F.R., Jimenez-Velez, B.D., 2010. Use of human bronchial epithelial cells (BEAS-2B) to study immunological markers resulting from exposure to PM2.5organic extract from Puerto Rico. Toxicology and Applied Pharmacology 243, 381–389. doi:10.1016/j.taap.2009.12.009

Genies, C., Jullien, A., Lefebvre, E., Revol, M., Maitre, A., Douki, T., 2016. Inhibition of the formation of benzo[a]pyrene adducts to DNA in A549 lung cells exposed to mixtures of polycyclic aromatic hydrocarbons. Toxicology in Vitro 35, 1–10. doi:10.1016/j.tiv.2016.05.006

Genies, C., Maître, A., Lefèbvre, E., Jullien, A., Chopard-Lallier, M., Douki, T., 2013. The extreme variety of genotoxic response to benzo[a]pyrene in three different human cell lines from three different organs. PLoS ONE 8, 1–11. doi:10.1371/journal.pone.0078356

Gualtieri, M., Longhin, E., Mattioli, M., Mantecca, P., Tinaglia, V., Mangano, E., Carla, M., Bestetti, G., Camatini, M., Battaglia, C., 2012. Gene expression profiling of A549 cells

exposed to Milan PM2 . 5. Toxicology Letters 209, 136–145. doi:10.1016/j.toxlet.2011.11.015

Gualtieri, M., Øvrevik, J., Mollerup, S., Asare, N., Longhin, E., Dahlman, H.J., Camatini, M., Holme, J.A., 2011. Airborne urban particles (Milan winter-PM2.5) cause mitotic arrest and cell death: Effects on DNA, mitochondria, AhR binding and spindle organization. Mutation Research - Fundamental and Molecular Mechanisms of Mutagenesis 713, 18–31. doi:10.1016/j.mrfmmm.2011.05.011

Happo, M.S., Uski, O., Jalava, P.I., Kelz, J., Brunner, T., Hakulinen, P., Mäki-Paakkanen, J., Kosma, V.M., Jokiniemi, J., Obernberger, I., Hirvonen, M.R., 2013. Pulmonary inflammation and tissue damage in the mouse lung after exposure to PM samples from biomass heating appliances of old and modern technologies. Science of the Total Environment 443, 256–266. doi:10.1016/j.scitotenv.2012.11.004

Henkler, F., Brinkmann, J., Luch, A., 2010. The role of oxidative stress in carcinogenesis induced by metals and xenobiotics. Cancers 2, 376–396. doi:10.3390/cancers2020376

Hukkanen, J., Lassila, A., Päivärinta, K., Valanne, S., Sarpo, S., Hakkola, J., Pelkonen, O., Raunio, H., 2000. Induction and regulation of xenobiotic-metabolizing cytochrome P450s in the human A549 lung adenocarcinoma cell line. American Journal of Respiratory Cell and Molecular Biology 22, 360–366. doi:10.1165/ajrcmb.22.3.3845

IARC: Outdoor air pollution a leading environmental cause of cancer deaths, 2013. 51, 229–235.

IARC Monographs on the Evaluation of Carcinogenic Risks to Humans, 2010. 95.

Jalava, P.I., Happo, M.S., Kelz, J., Brunner, T., Hakulinen, P., Mäki-Paakkanen, J., Hukkanen, A., Jokiniemi, J., Obernberger, I., Hirvonen, M.R., 2012. In vitro toxicological characterization of particulate emissions from residential biomass heating systems based on old and new technologies. Atmospheric Environment 50,

24–35. doi:10.1016/j.atmosenv.2012.01.009

Jin, W., Su, S., Wang, B., Zhu, X., Chen, Y., Shen, G., Liu, J., Cheng, H., Wang, X., Wu, S., Zeng, E., Xing, B., Tao, S., 2016. Properties and cellular effects of particulate matter from direct emissions and ambient sources. Journal of Environmental Science and Health - Part A Toxic/Hazardous Substances and Environmental Engineering 51, 1075–1083. doi:10.1080/10934529.2016.1198632

Kastan, M.B., Onyekwere, O., Sidransky, D., Vogelstein, B., Craig, R.W., 1991. Participation of p53 Protein in the Cellular Response to DNA Damage. Cancer Research 5, 6304–6311.

Kasurinen, S., Jalava, P.I., Happo, M.S., Sippula, O., Uski, O., Koponen, H., Orasche, J., Zimmermann, R., Jokiniemi, J., Hirvonen, M.R., 2017. Particulate emissions from the combustion of birch, beech, and spruce logs cause different cytotoxic responses in A549 cells. Environmental Toxicology. doi:10.1002/tox.22369

Kim, J.S., Peters, T.M., O'Shaughnessy, P.T., Adamcakova-Dodd, A., Thorne, P.S., 2013. Validation of an in vitro exposure system for toxicity assessment of air-delivered nanomaterials. Toxicology in Vitro. doi:10.1016/j.tiv.2012.08.030

Kocbach, A., Totlandsdal, A.I., Låg, M., Refsnes, M., Schwarze, P.E., 2008. Differential binding of cytokines to environmentally relevant particles: A possible source for misinterpretation of in vitro results? Toxicology Letters 176, 131–137. doi:10.1016/j.toxlet.2007.10.014

Kocbach Bølling, A., Pagels, J., Yttri, K.E., Barregard, L., Sallsten, G., Schwarze, P.E., Boman, C., 2009. Health effects of residential wood smoke particles: the importance of combustion conditions and physicochemical particle properties. Particle and fibre toxicology 6, 29.

Lamberg, H., Tissari, J., Jokiniemi, J., Sippula, O., 2013. Fine particle and gaseous emissions from a small-scale boiler fueled by pellets of various raw materials. Energy

and Fuels 27, 7044–7053. doi:10.1021/ef401267t

Li, Q., Jiang, J., Wang, S., Rumchev, K., Mead-Hunter, R., Morawska, L., Hao, J., 2017. Impacts of household coal and biomass combustion on indoor and ambient air quality in China: Current status and implication. Science of the Total Environment 576, 347–361. doi:10.1016/j.scitotenv.2016.10.080

Liang, Y., Lin, S.-Y., Brunicardi, F.C., Goss, J., Li, K., 2009. DNA Damage Response Pathways in Tumor Suppression and Cancer Treatment. World Journal of Surgery 33, 661–666. doi:10.1007/s00268-008-9840-1

Lindner, K., Ströbele, M., Schlick, S., Webering, S., Jenckel, A., Kopf, J., Danov, O., Sewald, K., Buj, C., Creutzenberg, O., Tillmann, T., Pohlmann, G., Ernst, H., Ziemann, C., Hüttmann, G., Heine, H., Bockhorn, H., Hansen, T., König, P., Fehrenbach, H., 2017. Biological effects of carbon black nanoparticles are changed by surface coating with polycyclic aromatic hydrocarbons. Particle and fibre toxicology 14, 8. doi:10.1186/s12989-017-0189-1

Longhin, E., Gualtieri, M., Capasso, L., Bengalli, R., Mollerup, S., Holme, J.A., Øvrevik, J., Casadei, S., Di Benedetto, C., Parenti, P., Camatini, M., 2016. Physico-chemical properties and biological effects of diesel and biomass particles. Environmental Pollution 215, 366–375. doi:10.1016/j.envpol.2016.05.015

Longhin, E., Pezzolato, E., Mantecca, P., Holme, J.A., Franzetti, A., Camatini, M., Gualtieri, M., 2013. Season linked responses to fine and quasi-ultrafine Milan PM in cultured cells. Toxicology in Vitro 27, 551–559. doi:10.1016/j.tiv.2012.10.018

Loxham, M., Morgan-Walsh, R.J., Cooper, M.J., Blume, C., Swindle, E.J., Dennison, P.W., Howarth, P.H., Cassee, F.R., Teagle, D.A.H., Palmer, M.R., Davies, D.E., 2015. The effects on bronchial epithelial mucociliary cultures of coarse, fine, and ultrafine particulate matter from an underground railway station. Toxicological Sciences 145, 98–107. doi:10.1093/toxsci/kfv034

Marabini, L., Ozgen, S., Turacchi, S., Aminti, S., Arnaboldi, F., Lonati, G., Fermo, P., Corbella, L., Valli, G., Bernardoni, V., Dell'Acqua, M., Vecchi, R., Becagli, S., Caruso, D., Corrado, L.G., Marinovich, M., 2017. Ultrafine particles (UFPs) from domestic wood stoves: genotoxicity in human lung carcinoma A549 cells. Mutation Research - Genetic Toxicology and Environmental Mutagenesis 820, 39–46. doi:10.1016/j.mrgentox.2017.06.001

Maréchal, A., Zou, L., 2013. DNA damage sensing by the ATM and ATR kinases. Cold Spring Harbor Perspectives in Biology 5, 1–17. doi:10.1101/cshperspect.a012716

Michael, S., Montag, M., Dott, W., 2013. Pro-inflammatory effects and oxidative stress in lung macrophages and epithelial cells induced by ambient particulate matter. Environmental Pollution 183, 19–29. doi:10.1016/j.envpol.2013.01.026

Muala, A., Rankin, G., Sehlstedt, M., Unosson, J., Bosson, J.A., Behndig, A., Pourazar, J., Nyström, R., Pettersson, E., Bergvall, C., Westerholm, R., Jalava, P.I., Happo, M.S., Uski, O., Hirvonen, M.-R., Kelly, F.J., Mudway, I.S., Blomberg, A., Boman, C., Sandström, T., 2015. Acute exposure to wood smoke from incomplete combustion - indications of cytotoxicity. Particle and Fibre Toxicology 12, 33. doi:10.1186/s12989-015-0111-7

Nemmar, A., Holme, J.A., Rosas, I., Schwarze, P.E., Alfaro-Moreno, E., 2013. Recent advances in particulate matter and nanoparticle toxicology: a review of the in vivo and in vitro studies. BioMed research international 2013, 279371. doi:10.1155/2013/279371

Pati, R., Das, I., Mehta, R.K., Sahu, R., Sonawane, A., 2016. Zinc-oxide nanoparticles exhibit genotoxic, clastogenic, cytotoxic and actin depolymerization effects by inducing oxidative stress responses in macrophages and adult mice. Toxicological Sciences 150, 454–472. doi:10.1093/toxsci/kfw010

Perrone, M.G., Gualtieri, M., Ferrero, L., Porto, C. Lo, Udisti, R., Bolzacchini, E., Camatini,

M., 2010. Seasonal variations in chemical composition and in vitro biological effects of fine PM from Milan. Chemosphere 78, 1368–1377. doi:10.1016/j.chemosphere.2009.12.071

Reyes-Zárate, E., Sánchez-Pérez, Y., Gutiérrez-Ruiz, M.C., Chirino, Y.I., Osornio-Vargas, Á.R., Morales-Bárcenas, R., Souza-Arroyo, V., García-Cuellar, C.M., 2016. Atmospheric particulate matter (PM10) exposure-induced cell cycle arrest and apoptosis evasion through STAT3 activation via PKCζ and Src kinases in lung cells. Environmental Pollution 214, 646–656. doi:10.1016/j.envpol.2016.04.072

Rossner, P., Strapacova, S., Stolcpartova, J., Schmuczerova, J., Milcova, A., Neca, J., Vlkova, V., Brzicova, T., Machala, M., Topinka, J., 2016. Toxic effects of the major components of diesel exhaust in human alveolar basal epithelial cells (A549). International Journal of Molecular Sciences 17. doi:10.3390/ijms17091393

Rudolf, E., Cervinka, M., 2011. Stress responses of human dermal fibroblasts exposed to zinc pyrithione. Toxicology Letters 204, 164–173. doi:10.1016/j.toxlet.2011.04.028

Samburova, V., Connolly, J., Gyawali, M., Yatavelli, R.L.N., Watts, A.C., Chakrabarty, R.K., Zielinska, B., Moosmüller, H., Khlystov, A., 2016. Polycyclic aromatic hydrocarbons in biomass-burning emissions and their contribution to light absorption and aerosol toxicity. Science of the Total Environment 568, 391–401. doi:10.1016/j.scitotenv.2016.06.026

Sànchez-Pérez, Y., Chirino, Y.I., Osornio-Vargas, A.R., Morales-Bàrcenas, R., Gutièrrez-Ruìz, C., Vàzquez-Lòpez, I., Garcìa-Cuellar, C.M., 2009. DNA damage response of A549 cells treated with particulate matter (PM10) of urban air pollutants. Cancer Letters 278, 192–200. doi:10.1016/j.canlet.2009.01.010

Secrest, M.H., Schauer, J.J., Carter, E.M., Lai, A.M., Wang, Y., Shan, M., Yang, X., Zhang, Y., Baumgartner, J., 2016. The oxidative potential of PM2.5 exposures from indoor and outdoor sources in rural China. Science of the Total Environment 571,

1477–1489. doi:10.1016/j.scitotenv.2016.06.231

Smith, J., Mun Tho, L., Xu, N., A. Gillespie, D., 2010. The ATM-Chk2 and ATR-Chk1 pathways in DNA damage signaling and cancer. Advances in Cancer Research 108, 73–112. doi:10.1016/B978-0-12-380888-2.00003-0

Stabile, L., Buonanno, G., Avino, P., Frattolillo, A., Guerriero, E., 2018. Indoor exposure to particles emitted by biomass-burning heating systems and evaluation of dose and lung cancer risk received by population. Environmental Pollution 235, 65–73. doi:10.1016/j.envpol.2017.12.055

Steenhof, M., Gosens, I., Strak, M., Godri, K.J., Hoek, G., Cassee, F.R., Mudway, I.S., Kelly, F.J., Harrison, R.M., Lebret, E., Brunekreef, B., Janssen, N.A., Pieters, R.H., 2011. In vitro toxicity of particulate matter (PM) collected at different sites in the Netherlands is associated with PM composition, size fraction and oxidative potential - the RAPTES project. Particle and Fibre Toxicology 8, 26. doi:10.1186/1743-8977-8-26

Strapáčová, S., Brenerová, P., Krčmář, P., Andersson, P., van Ede, K.I., van Duursen, M.B.M., van den Berg, M., Vondráček, J., Machala, M., 2018. Relative effective potencies of dioxin-like compounds in rodent and human lung cell models. Toxicology 404–405, 33–41. doi:10.1016/j.tox.2018.05.004

Sussan, T.E., Ingole, V., Kim, J.H., McCormick, S., Negherbon, J., Fallica, J., Akulian, J., Yarmus, L., Feller-Kopman, D., Wills-Karp, M., Horton, M.R., Breysse, P.N., Agrawal, A., Juvekar, S., Salvi, S., Biswal, S., 2014. Source of biomass cooking fuel determines pulmonary response to household air pollution. American Journal of Respiratory Cell and Molecular Biology 50, 538–548. doi:10.1165/rcmb.2013-0201OC

Swiston, J.R., Davidson, W., Attridge, S., Li, G.T., Brauer, M., Van Eeden, S.F., 2008. Wood smoke exposure induces a pulmonary and systemic inflammatory response in firefighters. European Respiratory Journal 32, 129–138. doi:10.1183/09031936.00097707

Torvela, T., Uski, O., Karhunen, T., Jalava, P., Sippula, O., Tissari, J., Hirvonen, M., Jokiniemi, J., 2014. Reference Particles for Toxicological Studies of Wood Combustion: Formation, Characteristics, and Toxicity Compared to Those of Real Wood Combustion Particulate Mass.

Totlandsdal, A.I., Øvrevik, J., Cochran, R.E., Herseth, J.I., Bølling, A.K., Låg, M., Schwarze, P., Lilleaas, E., Holme, J.A., Kubátová, A., 2014. The occurrence of polycyclic aromatic hydrocarbons and their derivatives and the proinflammatory potential of fractionated extracts of diesel exhaust and wood smoke particles. Journal of Environmental Science and Health - Part A Toxic/Hazardous Substances and Environmental Engineering. doi:10.1080/10934529.2014.854586

Uski, O., Jalava, P.I., Happo, M.S., Leskinen, J., Sippula, O., Tissari, J., Mäki-Paakkanen, J., Jokiniemi, J., Hirvonen, M.R., 2014. Different toxic mechanisms are activated by emission PM depending on combustion efficiency. Atmospheric Environment 89, 623–632. doi:10.1016/j.atmosenv.2014.02.036

Uski, O., Jalava, P.I., Happo, M.S., Torvela, T., Leskinen, J., Mäki-Paakkanen, J., Tissari, J., Sippula, O., Lamberg, H., Jokiniemi, J., Hirvonen, M.-R., 2015. Effect of fuel zinc content on toxicological responses of particulate matter from pellet combustion in vitro. The Science of the total environment 511, 331–40.

Uski, O.J., Happo, M.S., Jalava, P.I., Brunner, T., Kelz, J., Obernberger, I., Jokiniemi, J., Hirvonen, M.-R., 2012. Acute systemic and lung inflammation in C57Bl/6J mice after intratracheal aspiration of particulate matter from small-scale biomass combustion appliances based on old and modern technologies. Inhalation Toxicology 24, 952–965. doi:10.3109/08958378.2012.742172

Van Den Heuvel, R., Den Hond, E., Govarts, E., Colles, A., Koppen, G., Staelens, J., Mampaey, M., Janssen, N., Schoeters, G., 2016. Identification of PM10 characteristics involved in cellular responses in human bronchial epithelial cells

(Beas-2B). Environmental Research 149, 48–56. doi:10.1016/j.envres.2016.04.029

Wallach, D., Kang, T.-B., Kovalenko, A., 2013. Concepts of tissue injury and cell death in inflammation: a historical perspective. Nature Reviews Immunology 14, 51–59. doi:10.1038/nri3561

Yang, L., Liu, G., Lin, Z., Wang, Y., He, H., Liu, T., Kamp, D.W., 2016. Pro-inflammatory response and oxidative stress induced by specific components in ambient particulate matter in human bronchial epithelial cells. Environmental Toxicology 31, 923–936. doi:10.1002/tox.22102

Zhang, J., Ghio, A.J., Gao, M., Wei, K., Rosen, G.D., Upadhyay, D., 2007. Ambient Particulate Matter Induces Alveolar Epithelial Cell Cycle Arrest: Role Of G1 Cyclins. FEBS Lett 581, 5315–5320.

Zhang, J., Song, W., Guo, J., Zhang, J., Sun, Z., Ding, F., Gao, M., 2012. Toxic effect of different ZnO particles on mouse alveolar macrophages. Journal of Hazardous Materials 219–220, 148–155. doi:10.1016/j.jhazmat.2012.03.069

Graphical abstract

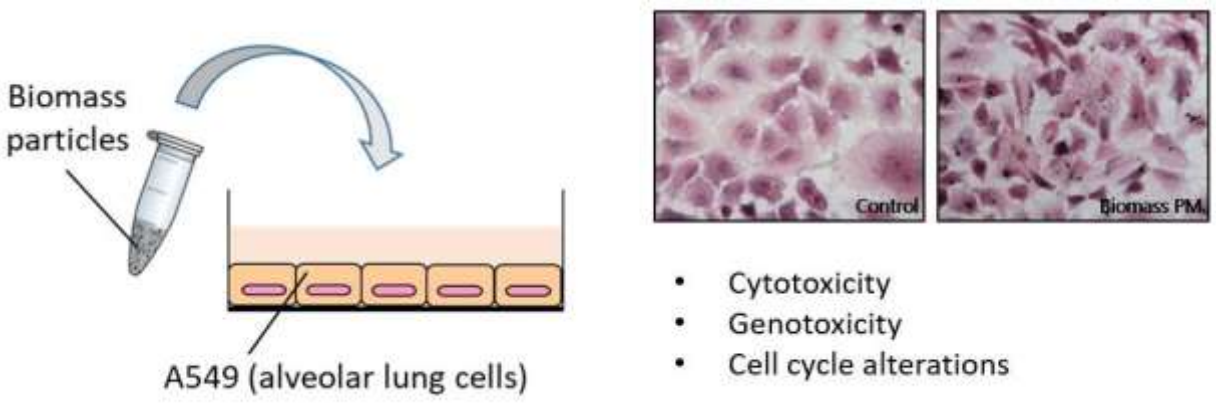

Highlights

- Biomass particles with diverse properties induce different biological responses
- Pellet PM with high metal content induce DNA damage and cell cycle alteration
- Elevated Zinc concentration cause cytotoxic and genotoxic effects